Finite Element Analysis of Laser-Generated Ultrasound for Characterizing Surface-Breaking Cracks

Hyunjo Jeong*

Division of Mechanical and Automobile Engineering, Wonkwang University, 344-2 Sinyong-Dong, Iksan, Jeonbuk 570-749, Korea

A finite element method was used to simulate the wave propagation of laser-generated ultrasound and its interaction with surface breaking cracks in an elastic material. Thermoelastic laser line source on the material surface was approximated as a shear dipole and loaded as nodal forces in the plane-strain finite element (FE) model. The shear dipole-FE model was tested for the generation of ultrasound on the surface with no defect. The model was found to generate the Rayleigh surface wave. The model was then extended to examine the interaction of laser generated ultrasound with surface-breaking cracks of various depths. The crack-scattered waves were monitored to size the crack depth. The proposed model clearly reproduced the experimentally observed features that can be used to characterize the presence of surface-breaking cracks.

Key Words: Finite Clement Analysis, Laser-Generated Ultrasound, Surface-Breaking Crack, Rayleigh Surface Wave, Shear Dipole Model, Crack Sizing

1. Introduction

Laser ultrasonics is a non-contact technique that is receiving growing attention because of its wide range of applicability in nondestructive evaluation (Scruby and Drain, 1990; Hutchins, 1988; Davies et al., 1993). The laser generation of ultrasound provides a number of advantages over the conventional generation by PZT transducers, namely high spatial resolution, broad-band generation, and ability to operate on curved locations. There are generally two mechanisms for such wave generation, depending on the amount of energy deposition by the laser pulse, namely ablation at very high power, and thermoelastic generation at moderate power operation. The latter does not damage the surface of the material, and is therefore suitable for applications in nondestructive evaluation. Ultrasound generated by laser irradiation contains a large component of surface wave motion, and is therefore particularly useful for the detection of surface-breaking cracks.

Traditional techniques for the detection of surface-breaking cracks rely on monitoring the reflection (pulse-echo) or the changes in the amplitude of the transmission (pitch-catch) of incident wave caused by the presence of a defect. Extensive investigations into the interaction of laser-generated Rayleigh waves with surface-breaking defects were conducted (Cooper et al., 1986). It was demonstrated that the crack size could be determined by the analysis of the time delay between the two peaks of the scattered Rayleigh pulse.

A large part of the modeling effort for laser generated ultrasound has relied on replacing the laser source with an equivalent set of stress boundary conditions (Scruby et al., 1990; Rose, 1984). This equivalent stress distribution, which takes the form of a shear stress dipole, has proven to be

* **E-mail** : hjjeong@wonkwang.ac.kr
TEL : +82-63-850-6690; **FAX** : +82-63-850-6691
Division of Mechanical and Automobile Engineering, Wonkwang University, 344-2 Sinyong-Dong, Iksan, Jeonbuk 570-749, Korea. (Manuscript **Received** October 6, 2004; **Revised** March 15, 2005)

extremely useful in describing many features of laser generated ultrasonic waveforms in thermoelastic regime. For instance, the epicentral waveform (Telschow and Conant, 1990), the surface acoustic waveform (Hurley et al., 1998), and the directivity pattern (Davies et al., 1993 ; Bernstein and Spicer, 2000) are all modeled accurately using a set of stress boundary conditions that are equivalent to a thermoelastic source.

In this paper, we apply a finite element method to simulate the observed interaction of laser generated ultrasound with surface breaking cracks. The fixed laser line source is considered, where the crack-scattered Rayleigh waves are monitored to characterize a crack. The thermoelastic laser line source is modeled as a shear dipole on the surface of a material and the effect of thermal diffusion is neglected. The subsequent propagation and scattering of elastodynamic waves are simulated using a finite element method. A commercial finite element package, ANSYS, was used in this work.

We first describe two important parameters, the element size and the integration time step, in the elastodynamic FE method. A shear dipole-FE model is then introduced to simulate the generation of ultrasound on the surface with no defect. The model is then extended to examine the interactions of laser generated ultrasound with surface-breaking cracks of 0.3−5.0 mm depth. Simulation results are provided and found to reproduce the significant features observed in the experiments.

2. Modeling for Thermoelastic Laser Generation of Ultrasound

2.1 Elastodynamic finite element analysis

Without viscous damping being considered, the finite element formulation of elastodynamic problem results in the discrete equations of motion given as

$$\mathbf{Ku}+\mathbf{M}\ddot{\mathbf{u}}=\mathbf{F}(t) \tag{1}$$

where $\mathbf{K}$ is the global stiffness matrix ; $\mathbf{M}$ is the mass matrix ; $\mathbf{F}$ is the vector of applied loads ; and $\mathbf{u}$ and $\ddot{\mathbf{u}}$ are the displacement and its second order time derivatives, respectively. The second order time derivative term has to be approximated in order to get a fully discretized formulation by which the displacement vector can be solved. The Newmark time integration scheme is chosen for this purpose (Moser et al., 1999).

Suitable time interval and element size are important for the accuracy of numerical solutions in finite element calculations involving wave propagation. The integration time step, Δt, is the time interval for which Eq. (1) is solved. The Newmark time integration scheme employs 20 points per cycle of $f_{\max}$ (ANSYS, 2000), where $f_{\max}$ is the highest frequency of interest :

$$\Delta t=\frac{1}{20f_{\max}} \tag{2}$$

For element size, l_e, it is generally recommended that 10 to 20 nodes per wavelength be used (ANSYS, 2000 ; Alleyne and Cawley, 1991), that is

$$l_e=\frac{\lambda_{\min}}{20}\sim\frac{\lambda_{\min}}{10} \tag{3}$$

where $\lambda_{\min}$ is the shortest wavelength involved.

Proper choice of Δt and l_e will satisfy the stability condition. This condition states that the wave should not propagate right across one mesh volume in a single time step :

$$\Delta t<\frac{l_e}{V_{L\max}} \tag{4}$$

where l_e is the smallest spacing between the nodes in the mesh and $V_{L\max}$ is the largest longitudinal wave velocity.

The FE program used in this work is ANSYS 5.6, a commercial, general-purpose FE code. A plane strain, 4-noded element model was constructed to simulate the propagation of a laser-generated ultrasound and its interaction with surface-breaking cracks.

2.2 Shear-dipole model

When a laser pulse radiates onto a solid surface, the surface region absorbs electromagnetic energy of the laser source which raises the surface temperature of the sample. The heated region undergoes rapid thermal expansion, causing ultra-

sonic wave generation. In this study, we shall restrict attention to the so-called thermoelastic regime. It is assumed that no significant optical penetration occurs below the surface of the test material. Furthermore, thermal diffusion is neglected as it is not a significant factor within the time scale of interest.

According to (Scruby and Drain, 1990), a thermoelastic source at a point in the interior of an isotropic material can be represented by three orthogonal force dipoles of equal strength. When the thermoelatic laser source is applied on the surface, it has been shown that the source becomes a surface center of expansion, which is equivalent to a pair of orthogonal dipoles parallel to the surface (Rose, 1984).

As the dipole strength is proportional to the laser induced temperature rise, the spatial and temporal temperature profiles at the surface should be specified. In this study, an infinitesimally thin line laser source is assumed. Under this assumption, the spatial variation of dipoles can be neglected and the surface center of expansion becomes a single shear dipole. The temporal distribution of the surface temperature is assumed to be a half cycle sinusoidal function, similar to that of the incident laser pulse (Ready, 1971).

Figure 1 shows the schematic of modeling process to simulate the thermoelastic laser generation of ultrasound. An infinitely long line laser pulse is radiated on the surface of a test specimen (Fig. 1(a)). The thermoelastic source is then replaced by a set of shear dipoles along the line source, leading to a plane strain formulation (Fig. 1(b)). A shear dipole is applied in the form of nodal forces of equal magnitude and opposite direction in the 2-D FE model as shown in Fig. 1(c).

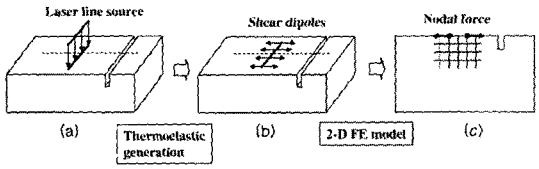

Fig. 1 Two dimensional FE modeling of thermoelastic laser generation of ultrasound: (a) Line-focused pulsed laser source, (b) Equivalent surface shear dipoles, and (c) 2-D plane strain FE model

2.3 Wave propagation analysis

In order to establish that the shear dipole approximation adequately models thermoelastic laser generation of ultrasound, a test case of an uncracked aluminum block is first considered. For the simulation a 40 mm×20 mm rectangle (in x and y direction respectively) is used as shown in Fig. 2. A symmetry boundary condition was applied at the left edge. The upper edge of the material on which the source is applied has a free boundary condition. The material used is aluminum, and its properties are: density $\rho=2600\ \text{kg/cm}^3$, longitudinal wave velocity $V_L=6300$ m/s, shear wave velocity $V_S=3100$ m/s, and Rayleigh wave velocity $V_R=2895$ m/s.

The shear dipole is applied on the upper left corner of the model as a nodal force in the x direction. The temporal pulse shape of the laser source is simply assumed to be a sinusoidal function. A 2 MHz half cycle sinusoidal wave is used for this purpose. In this case the wavelength of Rayleigh wave is $\lambda_R=1.45$ mm. According to the recommendations in the previous section, this problem is solved with an element size of 0.1 mm and an integration time step of 0.025 μs. A 2-D plane strain, 4-node isoparametric element is used.

Figure 2 is a snapshot at $t=0.3$ μs of the waves

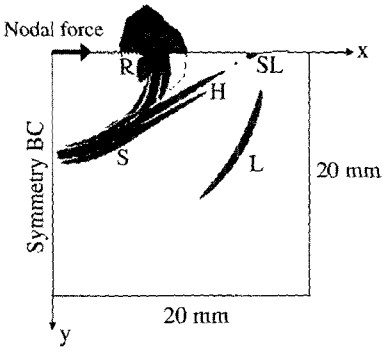

Fig. 2 Displacements snapshot using a shear dipole FE model for laser-generated ultrasound (material=aluminum, force function=$\sin 2\pi ft$ ($0\le t\le 0.25$ μs), $f=2$ MHz, element used=4 node isoparametric, $l_e=0.1$ mm, $\Delta t=0.025$ μs)

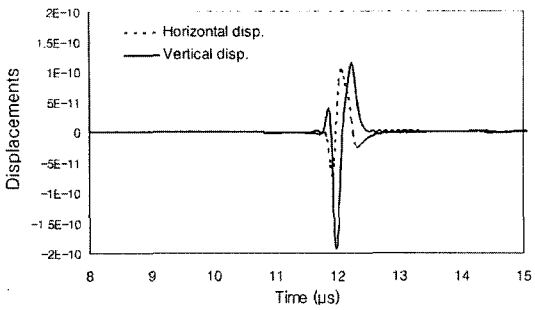

Fig. 3 Horizontal and vertical displacement components of Rayleigh wave on the surface at a location of $x=25\lambda_R$

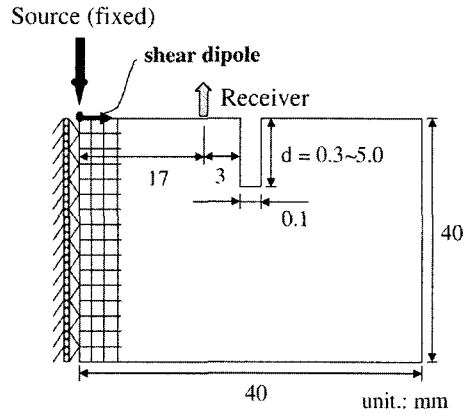

Fig. 4 Shear dipole-FE modeling of fixed laser source for investigating the interaction of laser-generated Rayleigh pulse with surface-breaking cracks (material=aluminum, force function=$\sin 2\pi ft$ ($0\leq t\leq 0.25$ μs), $f=2$ MHz, element used=4 node isoparametric, $l_e=0.1$ mm, $\Delta t=0.025$ μs)

generated by a half cycle sine function. From this figure, we can see that a total of five waves are generated, namely, skimming longitudinal wave (SL), head wave (H), bulk longitudinal wave (L), bulk shear wave (S), and surface wave (R). The skimming longitudinal wave propagates with longitudinal wave speed just underneath the free surface. A longitudinal and shear bulk waves also propagate toward the bottom and right edges of the model. The surface wave shows the largest displacement amplitude.

Figure 3 shows the time history of the horizontal and vertical displacement components on the surface at a location of $x=25\lambda_R$. Two waves are recorded at this point, one is skimming longitudinal wave (first arrival, not shown in the figure) and the other corresponds to the Rayleigh surface wave arriving later in time and both arriving at the theoretically predicted arrival time. We note in Fig. 3 that the horizontal displacement component lags behind the vertical displacement component. This time lag is a characteristic of Rayleigh surface wave. Therefore, it is concluded that the surface wave generated by the laser irradiation is the Rayleigh surface wave.

3. Interaction with Surface-Breaking Cracks

We consider the case where both laser source and receiver (optical interferometer) are fixed with respect to the crack. The FE model and the parameters used are shown in Fig. 4. These parameters are the same as those used in the previous section. The upper left corner of the specimen is loaded with a force boundary condition in the x direction. A half cycle sinusoidal wave with frequency 2 MHz was applied as a nodal force. The model is discretized using 15 elements per wavelength for the Rayleigh wave in aluminum at 2 MHz.

The surface-breaking crack is a 2-D machined slot, perpendicular to the surface of the half-space. The slot varies in depth between 0.3 and 5.0 mm, being 0.1 mm wide. This model is similar to the experimental arrangement of Cooper et al.(1986), where they studied the interaction of laser-generated ultrasound with machined slots.

Figure 5 shows the calculated time traces of vertical component for slot depths from 0.3 to 5.0 mm. We note that first there is a direct Rayleigh wave, whose time delay corresponds to the source-receiver separation. This wave is followed by a Rayleigh wave scattered from the crack. The scattered wave takes the form of two separate waves. From a detailed study of the wave-arrival times at the receiver, the first pulse has the characteristics of a Rayleigh wave reflected from the top corner of the crack. For the presence of the second pulse, Cooper et al.(1986) proposed a

model of diffraction from the lower crack tip and mode-conversion at the surface. A transmitted component of surface wave travels down the side wall and is diffracted at the tip mainly into shear wave. Some fraction scatters back to the surface at the critical angle and is mode converted to another Rayleigh wave, producing the second wave. This phenomenon is schematically represented in Fig. 6.

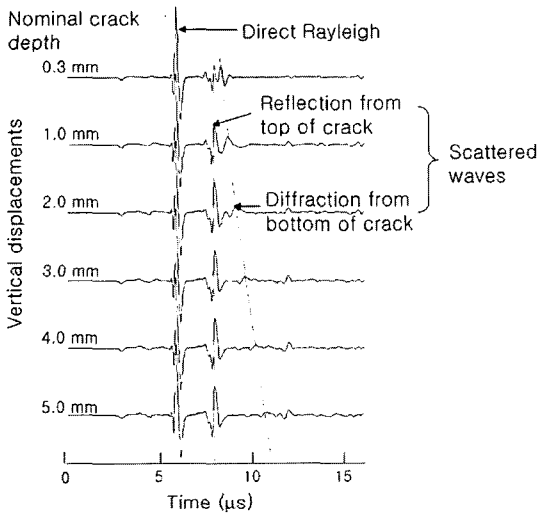

Fig. 5 Variation of scattered Rayleigh pulses with slot depth of 0.3-5.0 mm ; pulse-echo mode ; source-to-slot distance=20 mm, and receiver-to-slot distance=3 mm

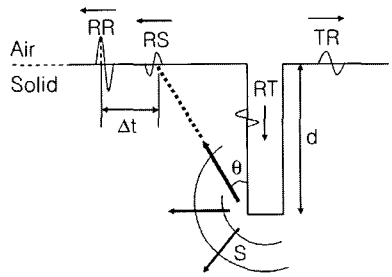

Fig. 6 Physical process involved when an incident Rayleigh pulse interacts with a slot to produce reflected and transmitted surface pulse (RR : Reflected Rayleigh pulse at top corner, RT : Rayleigh pulse transmitted around top corner, S : Diffracted shear wave at lower crack tip, RS : Rayleigh pulse resulting from the diffracted shear wave S at lower crack tip, TR : Transmitted Rayleigh pulse)

In Fig. 5, the separation between the two peaks in the scattered Rayleigh pulse clearly increases with slot depth. For a slot depth of 0.3 mm, the first and second peaks in the reflected pulse are just resolved, whereas for slot depths greater than 5.0 mm the amplitude of the second feature becomes almost indistinguishable. The time delay between the two peaks of the scattered Rayleigh pulse can be related to the crack depth, so this feature can be used for sizing the crack depth. The time difference between the RR and RS waves can be obtained as follows by considering the travel path and velocity of these waves :

$$t_D=\frac{d}{V_R}+\frac{d}{V_S\cos\theta}-\frac{d\tan\theta}{V_R} \tag{5}$$

If we use $\theta=30°$ for the critical angle (Cooper et al., 1986), the expression for the crack depth is given by

$$d=\frac{\sqrt{3}\,t_d V_R V_S}{(\sqrt{3}-1)\,V_S+2V_R} \tag{6}$$

Figure 7 shows a comparison of actually and ultrasonically measured crack depths. The agreement is found to be very good.

As illustrated thus far the proposed model clearly reproduces the interaction of laser-generated Rayleigh pulse with surface-breaking cracks observed experimentally (Cooper et al., 1986). Nevertheless, for small defects relative to

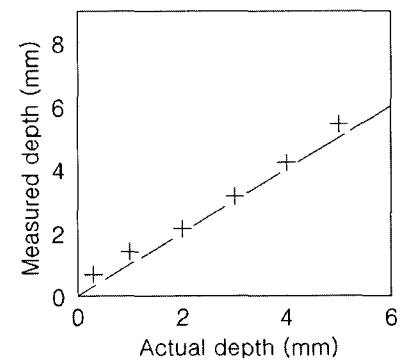

Fig. 7 A comparison of actually and ultrasonically measured slot depths

the wavelength of the generated Rayleigh wave, the scattered waves are often too weak to be detected. The recently proposed scanning laser source (SLS) technique provides an alternative inspection method which overcomes these size limitations (Kromine et al., 2000). The SLS approach is based on the monitoring changes in laser-generated ultrasound as a laser source is scanned over a defect. When the SLS is very close to a crack, due to scattering and changes in the conditions of generation of ultrasound, the amplitude of Rayleigh wave increases significantly, as compared to the signal generated when the SLS is far ahead or far behind the crack. These signatures are found to be noticeable even for cracks much smaller than the wavelength of incident Rayleigh wave.

4. Conclusions

A model for the laser-generated ultrasound for the detection and characterization of surface-breaking cracks has been presented. The generation of ultrasound by a line-focused laser source was modeled by a shear dipole acting on the surface of two dimensional isotropic solid. The subsequent propagation and scattering of generated waves were analyzed by the finite element method. The shear dipole-FE model provided correct Rayleigh wave displacement components when tested on the surface with no crack. The model clearly reproduced the far-field scattering phenomena experimentally observed in large surface -breaking cracks when the laser source was fixed far ahead of cracks.

Acknowledgments

This work was supported by Research Institute of Engineering Technology Development, Wonkwang University.

References

Alleyne, D. and Cawley, P., 1991, "A Two-Dimensional Fourier Transform Method for Measurement of Propagating Multimode Signals," *Journal of the Acoustical Society of America*, Vol. 89, No. 3, pp. 1159~1168.

ANSYS user's manual for revision 5.6, 2000, Swanson Analysis Systems, Houston, TX.

Bernstein, J. R. and Spicer, J. B., 2000 "Line Source Representation for Laser-Generated Ultrasound in Aluminum," *Journal of the Acoustical Society of America*, Vol. 107, No. 3, pp. 1352~1357.

Cooper, J. A., Dewhurst, R. J. and Palmer, S. B., 1986, "Characterization of Surface-Breaking Defects in Metals with the Use of Laser-Generated Ultrasound," *Philosphical Transactions on Royal Society of London*, Vol. A320, pp. 319~328.

Davies, S. J., Edwards, C., Taylor, G. S. and Palmer, S. B, 1993, "Laser-Generated Ultrasound: Its Properties, Mechanisms and Multifarious Applications," *Journal of Physics D : Applied Physics*, Vol. 26, 329~348

Hurley, D. H., Spicer, J. B., Wagner, J. W. and Murray, T. W., 1998, "Investigation of the Anisotropic Nature of Laser-Generated Ultrasound in Zinc and Unidirectional Carbon Epoxy Composites," *Ultrasonics*, Vol. 36, pp. 355~360

Hutchins, D. A., 1988, Ultrasonic Generation by Pulsed Lasers, Physical Acoustics, ed. W. P. Mason and R. N. Thurston, Vol. 18, Chap. 2, Academic Press, New York.

Kromine, A. K., Fomitchov, P. A., Krishnaswamy, S. and Achenbach, J. D., 2000, "Laser Ultrasonic Detection of Surface Breaking Discontinuities : Scanning Laser Source Technique," *Materials Evaluation*, Vol. 58, No. 2, pp. 173~177

Moser, F., Jacobs, L. J. and Qu, J., 1999, "Modeling Elastic Wave Propagation in Waveguides with the Finite Element Method," *NDT& E International*, Vol. 32, pp. 225~234.

Ready, J. F., 1971, "Effects of High-Power Laser Radiation," Academic Press, New York-, Chap. 3.

Rose, L. R. F., 1984, "Point-Source Representation for Laser-Generated Ultrasound," *Journal of the Acoustical Society of America*, Vol. 75, No. 3, pp. 723~732.

Scruby, C. B., Dewhurst, R. J., Hutchins, D. A.

and Palmer, S. B., 1980, "Quantitative Studies of Thermally Generated Waves in Laser-Irradiated Metals," *Journal of Applied Physics*, Vol. 51, No. 12, 6210~6216.

Scruby, C. B. and Drain, L. E., 1990, Laser Ultrasonics : Techniques and Applications, Adam-Hilger, New York.

Telschow, K. L. and Conant, R. J., 1990, "Optical and Thermal Parameter Effects on Laser-Generated Ultrasound," *Journal of the Acoustical Society of America*, Vol. 88, pp. 1494~1502.